



Effect of Using Different Property Modelling Strategies on the Calculated Value of the Initial Oil in Place by Volumetric Method

¹Jassim M. Al Said Naji*, ¹Mohammed A. Ahmed, ²Hijran M. Hammad, ³Ali M. Fadhil

¹Oil and Gas Engineering Department, University of Technology, Baghdad, Iraq

²Ministry of Oil, Mid. Land Oil Company, Iraq

³South west petroleum university (SWPU), China

Article information

Article history:

Received: August, 22, 2023

Accepted: October, 06, 2023

Available online: October, 08, 2023

Keywords:

Property modeling,
Initial oil in place,
Moving Average,
Sequential Gaussian Simulation,
Volumetric method

*Corresponding Author:

Jassim M. Al Said Naji

150100@uotechnology.edu.iq

Abstract

The initial oil in place (*IOIP*) is an important factor that controls economic planning for production and field life. Therefore, this parameter must be determined precisely and carefully. The present paper is dealt with study the impact of adopting two different strategies of property modeling on *IOIP* value. 3D geological model constructed by using information likewise: contour map, oil formation volume factor, control processing interpretation (*CPI*) of well logs, and well heads and tops of twelve wells for selected field. The chosen oil field is feeding from Mishrif reservoir and located in southern Iraq. Mishrif reservoir is classified to six layers: MA, MB11, MB12, MB21, MC1, and MC2. Two strategies for distributing petrophysical properties: porosity, water saturation, and net to gross thickness of Mishrif reservoir are utilized. The two strategies are sequential Gaussian simulation and moving average. The volumetric method is used for estimating *IOIP* values. The impact of using the two strategies of property modeling was very clear where the values of *IOIP* had a significant difference. The *IOIP* value of 3D model whose petrophysical properties are distributed using moving average strategy is 5.145 billion barrels, while the 3D model distributed by Gaussian strategy had *IOIP* equal to 4.195 billion barrels. According to obtained results, the choice of distribution method is very important in estimation of *IOIP*. Selection of optimal property modeling strategy need to statistical comparison with selected oil field reports and input data, so finally, the closest representation of a protective reservoir and accurate value of *IOIP*.

DOI: <http://doi.org/10.55699/ijogr.2023.0302.1051>, Oil and Gas Engineering Department, University of Technology-Iraq

This is an open access article under the CC BY 4.0 license <http://creativecommons.org/licenses/by/4.0>

1. Introduction

One of the critical issues facing the petrophysics engineer is estimating the accurate initial oil in place (*IOIP*) contents that were present in the reservoir and assessing how much hydrocarbon can be recovered quantitatively from a field, zone, or area [1], as well as reservoir simulation and efficiency of fluid flow [2]. Science of oil and

gas engineering has the most extreme of uncertainty according to its dealing with things that are invisible or invincible, in addition to this issue, the utilized information for determination process causes the uncertainty problems and make it prevalent [3]. Numerous methods exist for estimating the amount of *IOIP*, including the volumetric method, the material balance method, the decline curve analysis method, and the simulation method [4]. The volumetric method is one from many methods used for determining *IOIP* and based on petrophysical properties data such as porosity, water saturation and net pay thickness [5]. The property modeling is the distribution of input petrophysical properties on related reservoir to get the closest representation of the actual reservoir [6]. Diagenesis, facies alteration and geostatistical are three examples of the various processes that lead to the property modeling and distribution of petrophysical properties in reservoir layers, therefore, building of geological model led to simulate definitely relevant petrophysical properties provide some insight into how these properties are modeled [7], another clarification, geological model can be defined a best understanding for how the hydrocarbon and rock properties distributed on reservoir layers [8]. In present paper the geostatistical modeling is adopted for property modeling, and it is representing as multi strategies used for reservoir characterization and it can be interpreted by utilizing the statistical parameters [9]. In order to analyze spatially distributed data, geostatistics applies the theory of random functions. It has been more than thirty years since geostatistical techniques like kriging made a comeback in the world of mainstream statistics. These techniques were originally developed for mining and petroleum exploration. The geostatistical methodology can be further divided into four categories: linear and multivariate geostatistics, non-stationary geostatistics, non-linear geostatistics, and geostatistical simulation [10]. Many alternative strategies for estimating and distributing petrophysical properties are used in geostatistical modeling, including various Gaussian, kriging and moving average strategies [11]

The objective of present paper is a study the effect of using two different strategies of geostatistical modelling for petrophysical properties: porosity, water saturation and net to gross thickness, on estimated values of *IOIP* by constructing two 3D geological models, one model for each geostatistical strategy of one southern Iraqi oil field that fed by Mishrif reservoir.

1.2. Area of Study and Reservoir Describing

The X oil field is located in southern Iraq, near to the Iranian border, 40 kilometers northeast of Amara, as seen in Fig. 1. The field was first identified in 1970, and its developmental stage began in 1976. The X oil field is part of the Mesopotamian Basin zone, which is unstable [12]. In southern Iraq, the Mishrif Formation is a significant reservoir. In actuality, the construction of X field consists of two domes, north and south domes. The north dome has a long 16 km and width 6 km, whereas the south dome has a long 23 km and width 8 km as shown in Fig. 2 [13]. Two reservoirs, the Khassib reservoir at the top and the Rumaila reservoir at the bottom, represent the boundaries of the Mishrif reservoir [14]. Mishrif reservoir is mostly composed of limestone and dolomite with interbedded shale, specifically near the top of the reservoir. A carbonate platform ramp may be seen in the Mishrif reservoir depositional environment [15]. Mishrif reservoir is comprised on Rudist, coral-reef, organic detrital limestone, shallow open-marine, and lagoonal facies [16] [17]. Mishrif reservoir had been classified into six layers (MA, MB11, MB12, MB21, MC1, and MC2) according to spatial variation of rock properties [14].

The Tertiary and Cretaceous are the two sequences that together make the stratigraphic column that penetrated in the X oil field. The structures from younger to older are a representation of tertiary time while Cretaceous is comprised on numbers of reservoirs as illustrated in Fig. 3 [18].

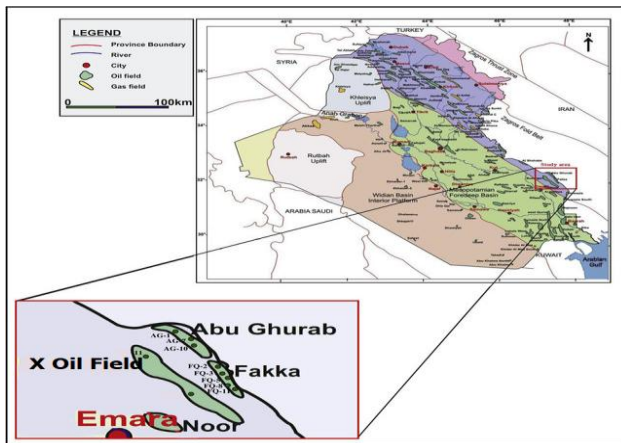


Figure 1: Location of X oil field on Iraq map [19].

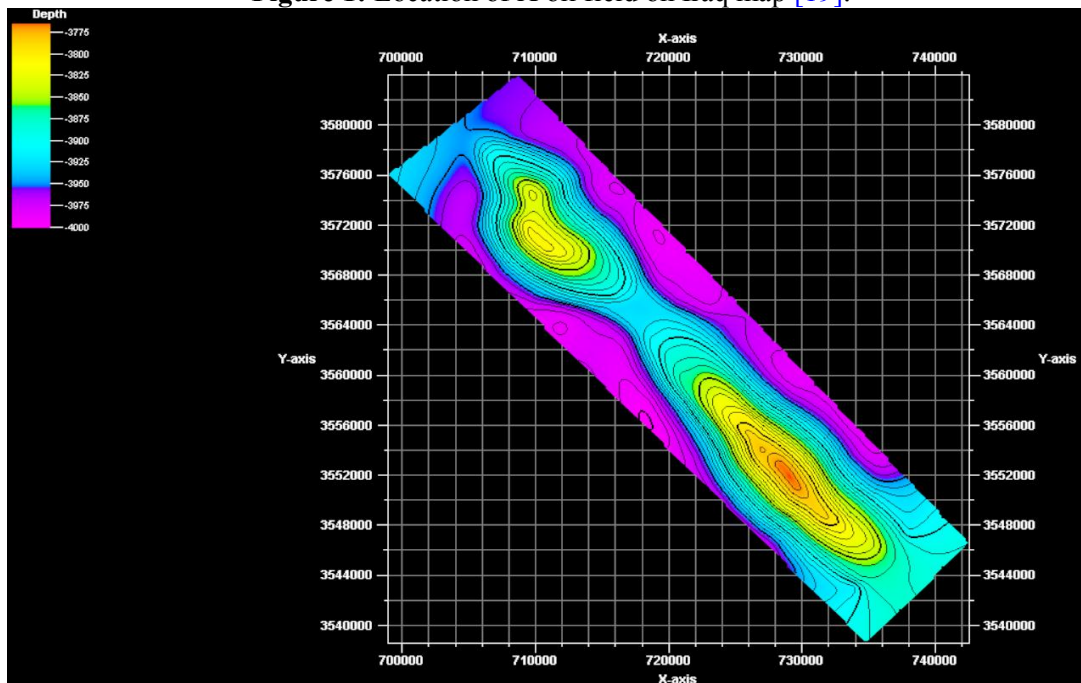


Figure 2: North and south domes of X oil field illustrated in contour map of MB21 top.

	Age	Formation	Lithology	Note	
Tertiary	Pliocene	Bakhtiary	Marly clay + Gypsum + Sandy clay		
	Upper Miocene	Upper Fars	Gravel Sand + Siltstone + Anhydrite + Shale		
	Middle Miocene	Lower Fars – MB5		Shale + Anhydrite + Limestone + Dolomite	
		Lower Fars – MB4		Shale + Anhydrite + Salt + Limestone	
		Lower Fars – MB3		Anhydrite + Salt + Shale	
		Lower Fars – MB2		Salt	
		Lower Fars – MB1		Anhydrite + Shale + Dolomite	
	Burdigalian	Jeribe/Euphrates	Limestone + Dolomite		
	Aquitanian to Oligocene	Upper Kirkuk		Sand + Siltstone + Shale + Dolomite	Asmari Formation
		M-L Kirkuk		Sand + Siltstone + Shale	
Eocene to Paleocene	Jaddala		Limestone + Marl + Chert + Shale		
	Aaliji		Marl + Limestone		
Cretaceous	Lower Maastrichtian	Shiranish	Chalky Limestone		
		Hartha	Chalky Limestone		
	Campanian to Santonian	Sadi	Limestone + Marl		
	Coniacian to Turonian	Tanuma	Shale + Marl + Limestone		
		Khasib	Limestone + Shale	Unconformity	
	Lower Turonian to Upper Cenomanian	Mishrif	Limestone		
		Rumaila	Limestone		
	Lower Cenomanian	Ahmedi	Marl + Limestone		
Mauddud					
	Nahr Umr				

Figure 3: Stratigraphic column of X oil field [17].

2. Materials and Methods

The existing study is performed by using data of twelve wells. The used data comprised on contour map of top of MB21 layer, computer processing interpretation (CPI) of logs which consisted from porosity, water saturation and net to gross thickness, well heads and tops and water oil contacts of each layer. The work methodology comprised on main four parts: data preparation, making 3D surface skeleton, scale up and property modelling, and at last volume calculation by volumetric method.

2.1. Data Preparation

The contour map of MB21 layer is digitized by using one of commercial softwares, the digitizing points were 10765. The well heads and tops are made according to Mishrif reservoir classification and well reports as shown in the following figure.

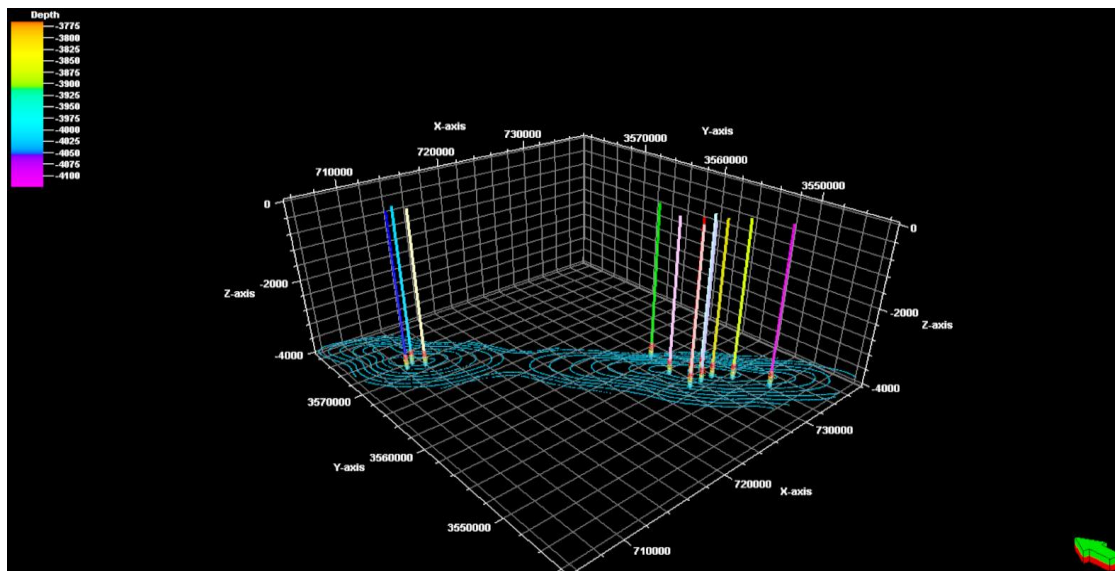


Figure 4: Digitized contour map and well heads and tops of twelve wells.

The used *CPI* in present paper of twelve oil wells that produced from Mishrif reservoir consisted from porosity, water saturation, and net to gross thickness. The *CPI* data was arranged, analyzed, and illogical values were removed and it summarized as shown in the **table 1** with east-west and south-north coordinates of each well.

Table 1: Summary of *CPI* logs and coordinates of twelve wells.

Well name	East-West Coordinate	North-South Coordinate	Mean of Porosity	Mean of Water Saturation	Mean of Net to Gross
Y1	711075.1931	3571610.961	0.093	0.0607	0.4169
Y2	730655.4501	3551234.13	0.0718	0.3536	0.4612
Y3	727094.0009	3555351.707	0.0719	0.6783	0.5291
Y4	728087.8123	3552586.913	0.1119	0.6344	0.44
Y5	729460.0713	3553790.868	0.0825	0.6343	0.4989
Y6	711839.2636	3570618.849	0.0961	0.6824	0.6086
Y7	726794.0553	3552701.551	0.0938	0.5617	0.58
Y8	732025.8926	3548351.333	0.0921	0.5291	0.4702
Y9	710226.4919	3571027.83	0.0937	0.5808	0.6555
Y10	727952.9614	3558386.46	0.1174	0.5661	0.5812
Y11	729390.5527	3552496.918	0.0797	0.5291	0.5161
Y12	728180.0956	3553856.515	0.1148	0.5186	0.6527

After analysing the *CPI* data, the depths of water oil contact (*WOC*) of each layer were determined based upon *CPI* interpretation and they summarized in the following **table 2**.

Table 2: Water oil contact of each layer.

Layer Name	WOC Depth (m)
MA	3764
MB11	3790
MB12	3800
MB21	3908
MC1	3922
MC2	3993

2.2. 3D Surface Skelton

The prepared data is inputted so the 3D model can be constructed. The first step of model construction is making 3D skeleton. Skelton is the classification of reservoir into many boxes with determined dimensions and each box has a single value of porosity, water saturation and net to gross [20]. The dimensions of each box (grid) of constructed 3D skeleton are 1000ft long and 1000ft width. Making horizons is the process of filling vertical thickness between layers' tops. This vertical thickness must be divided into numbers of sub layers according to reservoir heterogeneity and hydrocarbon content [21]. The number of sub layers of Mishrif reservoir is illustrated in [table 3](#), and this classification according to evaluation of Mishrif reservoir based on CPI logs.

Table 3: Number of sub layers between main layers' tops.

Vertical Thickness Between Two Layers	Number of Sub Layers
MA – MB11	10
MB11 – MB12	10
MB12 – MB21	15
MB21 – MC1	30
MC1 – MC2	25

2.3. Making Scale Up Property Modelling

The entered petrophysical properties: porosity, water saturation and net to gross thickness of twelve wells are averaged and these process is called scale up. The averaging process is accomplished by making the different values of each petrophysical properties related to each sub layer as a single value, so the accuracy of scale up is depending upon number of sub layers' classification. There are many types of averaging such as arithmetic, harmonic and geometric [22]. The adopted type is arithmetic mean averaging. [Figs. 5, 6, and 7](#) is displaying the scale up of entered properties of twelve wells.

Property modelling is the process of distributing each property from mentioned previously in each grid cell by using different geostatistical strategies such as sequential Gaussian simulation and moving average strategies. In these strategies, number of mathematical algorithms and tools are applied to determine the spatial variation of modelled property [23].

Sequential Gaussian Simulation Strategy is a popular strategy that has recently been embraced. Simply put, the fundamental characteristics of this strategy are flexibility and reasonability. It is based on Kriging strategy. The Kriging algorithms make it possible to take into account the correlation between the estimation and the collected data and to adhere to the provided variogram model, but they do not regulate such a correlation between any two estimates. Due to the smoothing effect, they frequently exaggerate tiny values or underestimate large values. As a result, sequential Gaussian simulation is created within a stochastic framework to solve this problem and offer other solutions [24]. The procedure of using the Sequential Gaussian Simulation Strategy in briefly is: (1) beginning with transforming the property data to normal distribution and (2) provide the Kriged guess, (3) after that the randomly seeds is putting on reservoir, and (4) the calculation process will begin in grids between putted seeds, (5) there are a number of values will represent a residual from normal distributed values and these will be under number of steps to reach the estimation process. The estimation of property will be according spatial variation [11].

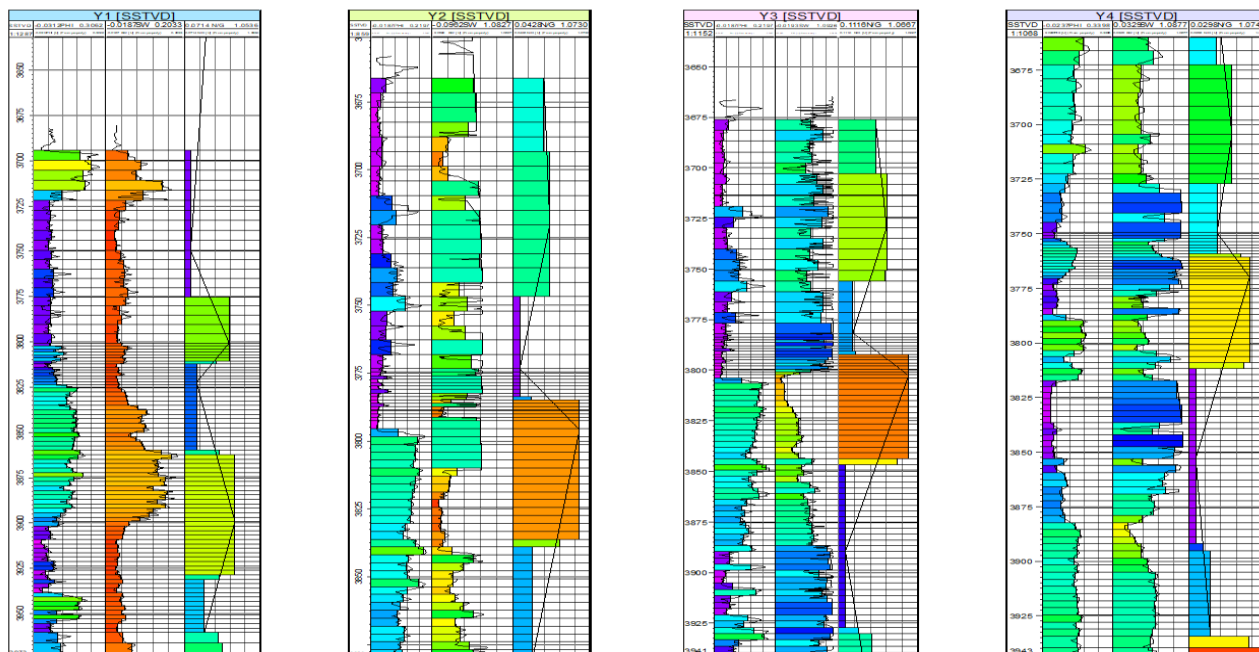


Figure 5: Porosity, water saturation, and net to gross thickness scale up of wells Y1, Y2, Y3, and Y4.

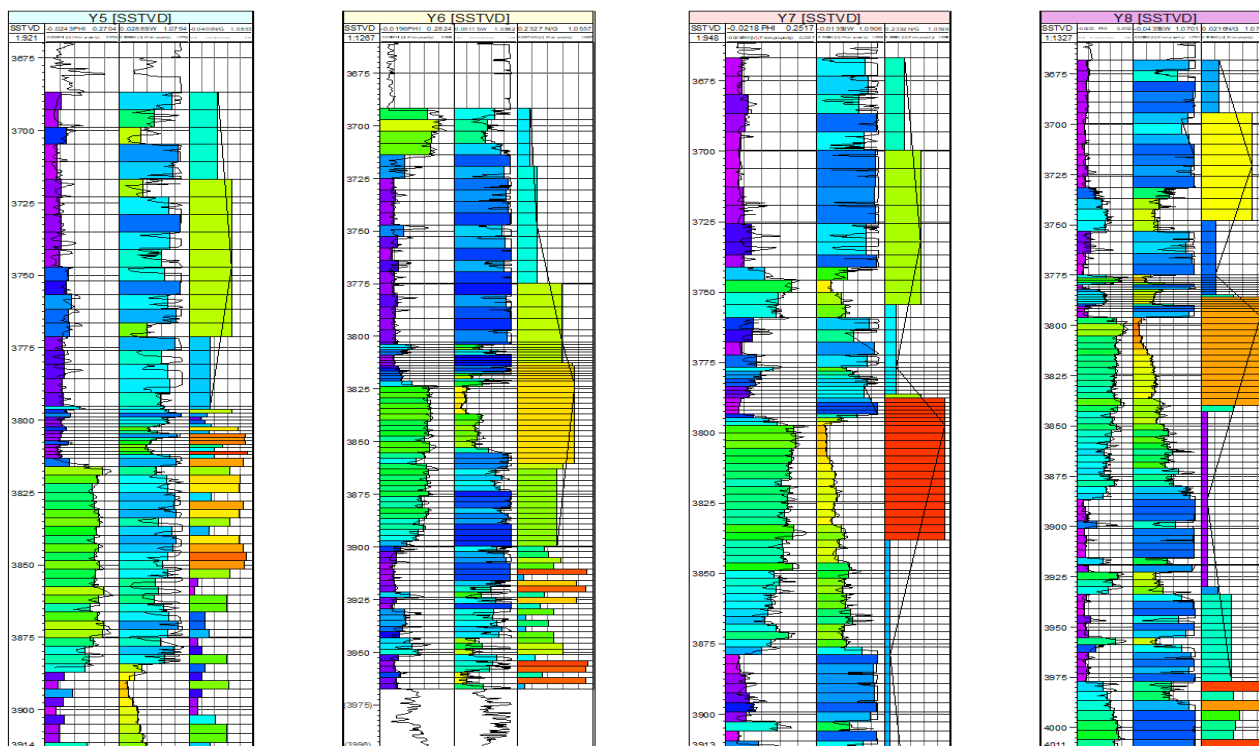


Figure 6: Porosity, water saturation, and net to gross thickness scale up of wells Y5, Y6, Y7, and Y8.

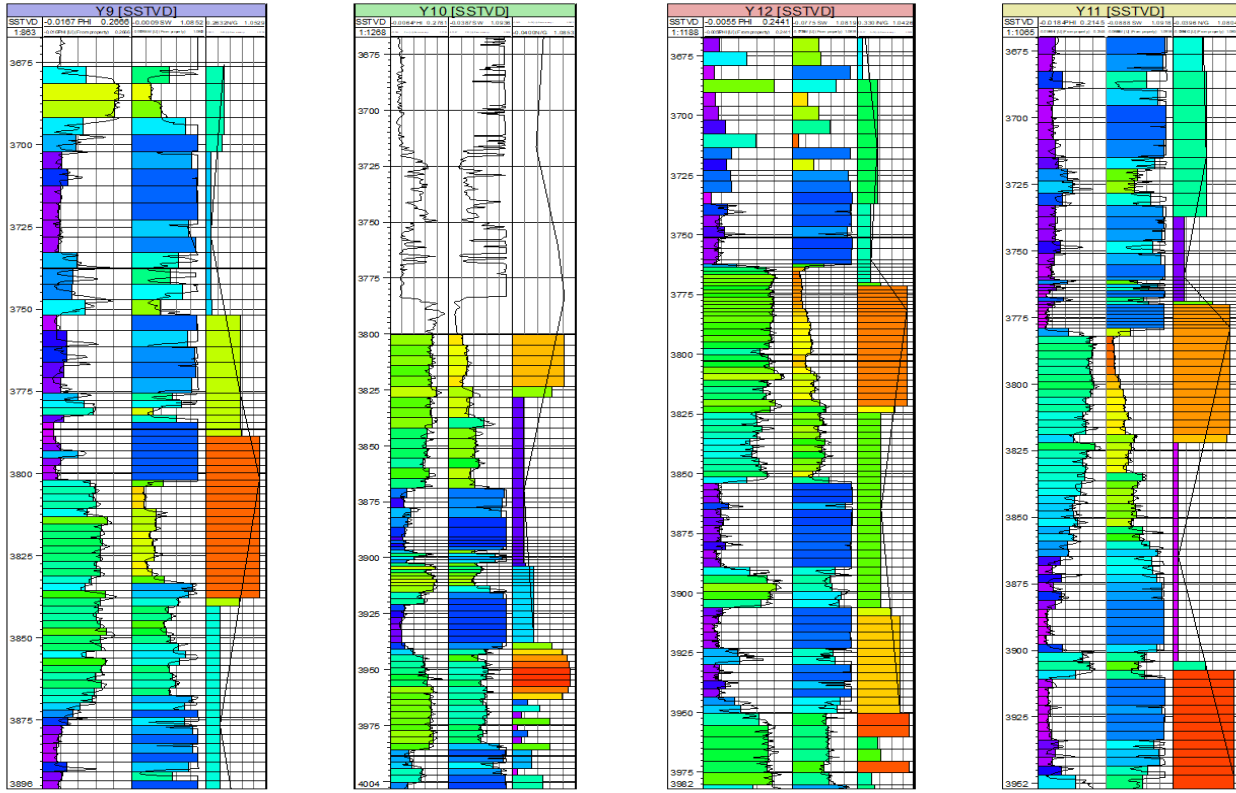


Figure 7: Porosity, water saturation, and net to gross thickness scale up of wells Y5, Y6, Y7, and Y8.

Moving Average Strategy: Calculates the input data's average and adjusts the weights for the wells' locations. The procedure is quick and will output values for each cell. When the input data span a wide range, it may also produce "bull's eyes." The method won't produce numbers that are either larger or lower than the min/max values of the input data as in the following equation [25]:

$$P(x,y,z) = \frac{1}{w} \sum wi . qi \tag{1}$$

Where:

(x,y,z): is the location of the cell center.

qi: are the upscaled cell values included in the summation.

wi: are the weighting values, and W is the sum of all the weights, which forces the effective sum of the weights to be one.

The distributions of porosity, water saturation, and net to gross thickness by sequential Gaussian simulation strategy are showing in **Fig. 8, 9, and 10**, while The distributions of porosity, water saturation, and net to gross thickness by moving average strategy are displaying in **Figs. 11, 12, and 13**.

2.7. Volumetric Method

The *IOIP* can be calculated by this method directly by exploration because this method need mainly to reservoir volume and some of petrophysical properties [13]. The volumetric method requires the reservoir's dimensions, the volume of the pores inside the rock matrix, and the fluid content of the void. This will give a precise estimate of the hydrocarbons present, from which the recovery factor can be used to determine the ultimate recovery [26]. The *IOIP* can be estimated by applying the following equation:

$$IOIP = \frac{7758 \times V_{bulk} \times \phi \times (1 - S_{wi})}{B_{oi}} \tag{2}$$

Where:

$IOIP$: is the initial oil in place (STB).

V_{bulk} : is a bulk volume of reservoir (Acre.ft).

ϕ : is the cell porosity (percent).

S_{wi} : is the in initial water saturation on each cell (percent)

B_{of} : is the oil formation volume factor (bbl/STB)

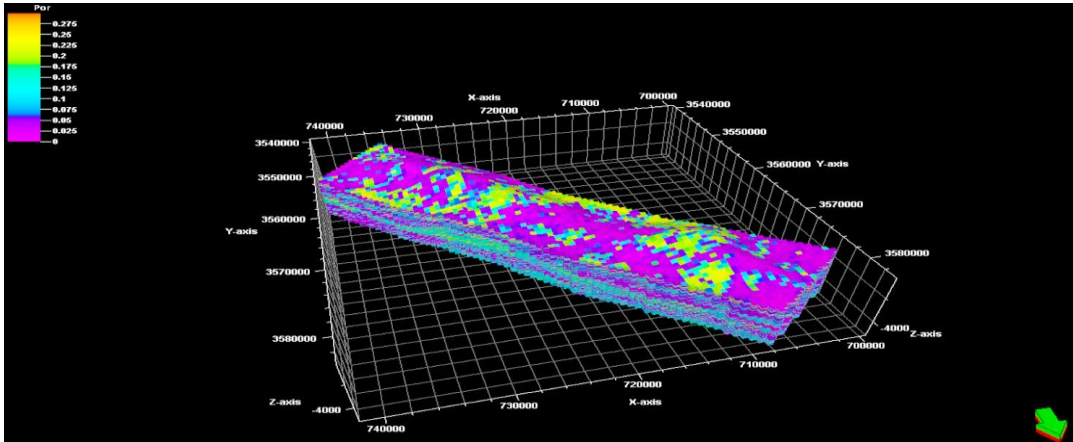


Figure 8: Porosity distribution on Mishrif layers by Gaussian sequential simulation strategy.

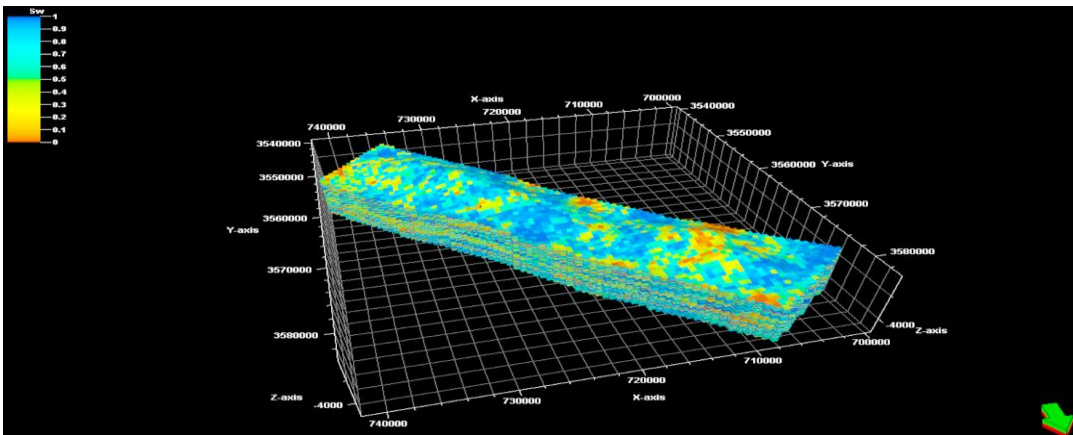


Figure 9: Water saturation distribution on Mishrif layers by Gaussian sequential simulation strategy.

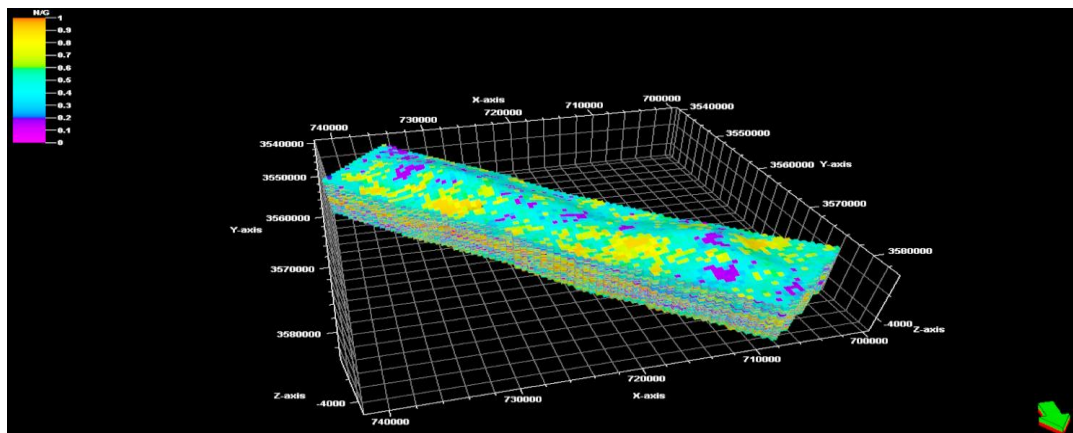


Figure 10: Net to Gross distribution on Mishrif layers by Gaussian sequential simulation strategy.

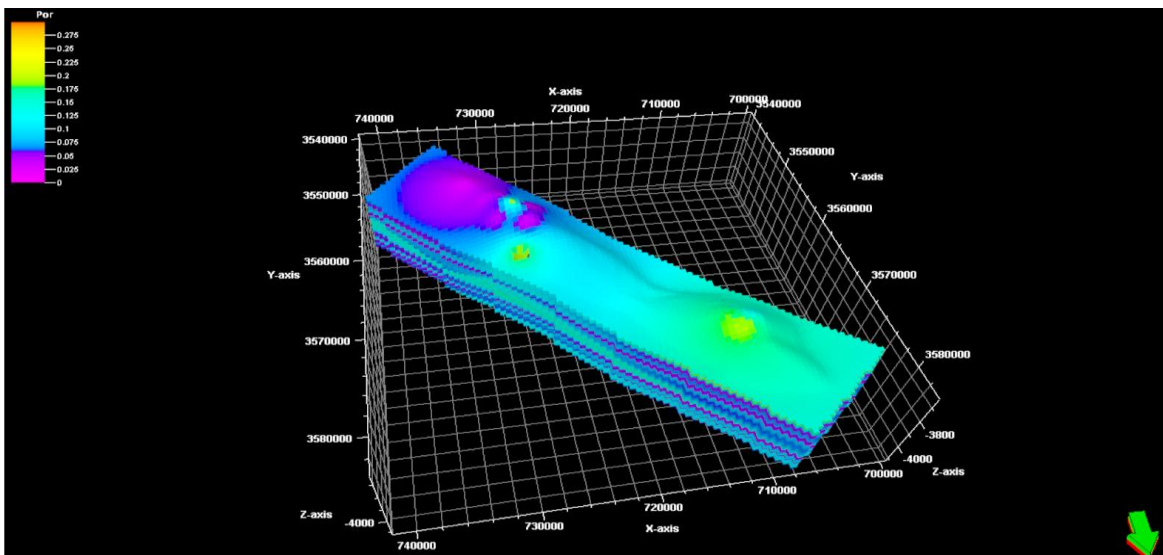


Figure 11: Porosity distribution on Mishrif layers by moving average strategy.

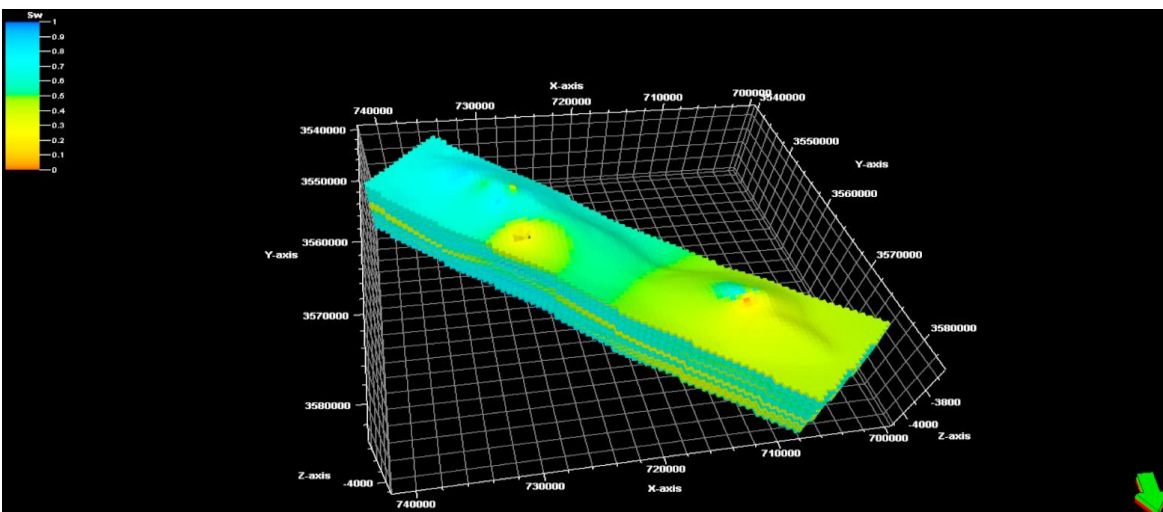


Figure 12: Water saturation distribution on Mishrif layers by moving average strategy.

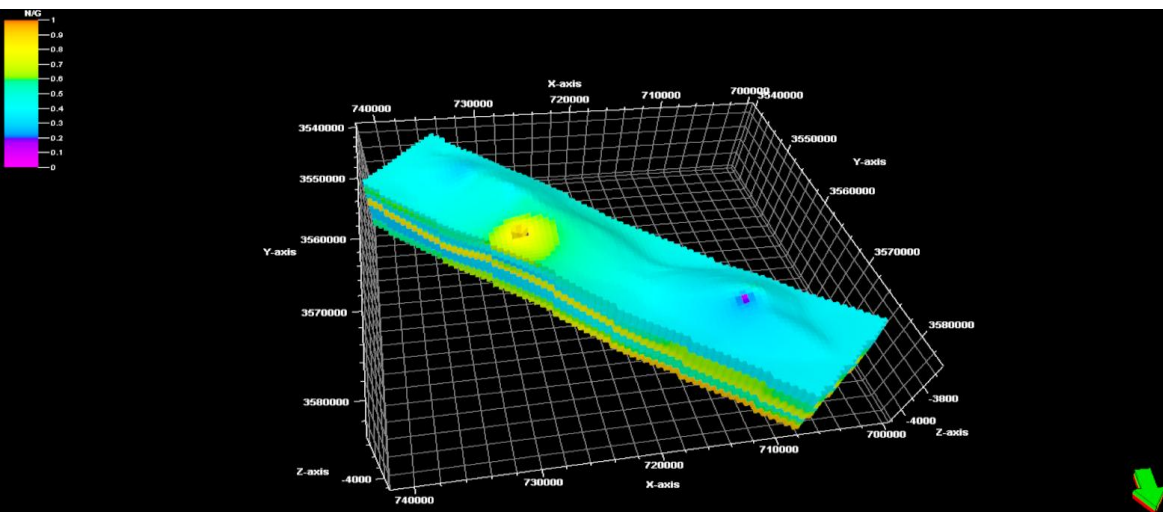


Figure 13: Net to Gross distribution on Mishrif layers by moving average strategy.

3. Results and Discussion

The two 3D geological models as illustrated in previous section parts were built. These two models had the same inputs but the difference between them the distributed strategies of porosity, water saturation and net to gross of Mishrif reservoir. This approach was achieved in order to proof the objective of the present paper. The *IOIP* is calculated by mentioned volumetric method which was represented by the eq.1 for the two constructed models. The results of *IOIP* for each layer of Mishrif reservoir of two models is summarizing in the following table:

Table 4: *IOIP* of Mishrif layers of two 3D constructed models.

Constructed 3D Model Based on Sequential Gaussian Simulation Strategy		Constructed 3D Model Based on Moving Average Strategy	
Layer	<i>IOIP</i> Value (MMSTB)	Layer	<i>IOIP</i> Value (MMSTB)
MA	660.43	MA	855.414
MB11	283.041	MB11	364.809
MB12	69.1879	MB12	62.8981
MB21	2786.39	MB21	3371.34
MC1	88.0574	MC1	94.3472
MC2	308.201	MC2	226.433
Total = 4195.3 MMSTB		Total = 5145.07 MMSTB	

The results in above **Table 4** are proofing the effect of difference in distribution strategy of petrophysical properties on *IOIP* values, where the quite difference between two models in *IOIP* values is very clear. This difference reaches to one billion STB and this value represents a great economic value that has a great return or loss if it is estimated incorrectly, as well as the value of *IOIP* is very important to determine accurately because it entails economic matters, determining the volumes of production, predicting the behaviour of the future reservoir performance, and developing development plans.

The current results are not subject to comparison because the main purpose is to know the effect of the different strategy of distribution on the reserve and this has been achieved, but the selection of the optimum strategy of property modelling depend on various parameters such as reservoir heterogeneity, trend of input data, type of available data, preparation of data approaches such as digitizing accuracy and interpretations, and number of wells on model. Based on these reasons and parameters the method of distribution properties will determine as geostatistical strategies, facies models or any modern approaches like artificial intelligence, so the optimum distributing of properties will obtain and the optimum *IOIP* will provide. If we want to set a value of *IOIP* for comparison, it is close to the results of the last study referred to in [14] carried out on the same field, reservoir and method that was equal to 4598 billion STB and the minor differences are very likely due to the different in distribution strategies and data used.

4. Conclusions

1. Two 3D geological models had been constructed by using the same input data of twelve wells of X oil field with single difference as a strategy of distributing of porosity, water saturation, and net to gross thickness.
2. The adopted two petrophysical properties distributing strategies are sequential Gaussian simulation and moving average.
3. The obtained results from two 3D models had a different in *IOIP* reach to one billion STB and this value has a significant economic effect in return or loss if estimated incorrectly.

4. The selection of approach of property modelling depend on various parameters so must be determined accurately to obtain optimum value of *IOIP*.

Nomenclature

(x,y,z): The location of the cell center.

B_{oi} : Oil formation volume factor (bbl/STB)

CPI: computer processing interpretation

IOIP: Initial oil in place (STB)

IOIP: Initial oil in place (STB).

\emptyset : Porosity (percent).

q_i : The upscaled cell values included in the summation.

S_{wi} : Initial water saturation on each cell (percent)

V_{bulk} : Bulk volume of reservoir (Acre.ft).

w_i : The weighting values, and W is the sum of all the weights, which forces the effective sum of the weights to be one.

WOC: Water oil contact (m)

References

- [1] M. Y. Nazarenko, "Probabilistic production forecasting and reserves estimation in water flooded oil reservoirs", Texas A&M University, published Thesis, USA. 2016.
- [2] A. M. Ali, and A. A. Alrazzaq, "Applying Facies Characterization to Build 3D Rock-Type Model for Khasib Formation, Amara Oil Field," Iraqi Journal of Oil & Gas Research, vol. 3, no. 1, pp. 94-105, 2023.
- [3] M. Najeeb, F. S. Kadhim, G. N. Sead, "Using Different Methods to Predict Oil in Place in Mishrif Formation / Amara Oil Field," Iraqi Journal of Chemical and Petroleum Engineering, vol. 21, no. 1, pp. 33-38, 2020.
- [4] A. O. Nasar, J. Abusaleem, E.M. Tabar, "Estimation of original oil in place for belhedan oil field by using volumetric method, material balance equation method, and reservoir simulation method," AIJR Publisher in Proceedings of First Conference for Engineering Sciences and Technology, pp. 298-309, 2018.
- [5] S. Ahmed, K. Elwegaa, M. Htawish, and H. Alhaj, "Determination of the oil initial in place, reserves, and production performance of the Safsaf C Oil Reservoir," International Journal of Engineering and Science, vol. 12, pp. 86-97, 2019.
- [6] R. Ahmed, S. M. Hamd-Allah, "Geological Model for Mauddud Reservoir in Khabaz Oil Field, Kirkuk, northern Iraq," Iraqi Geological Journal, vol. 54, no. 1D, 2021.
- [7] G. C. Abd Aoun, and T. A. Mahdi, "Geological model of Hartha formation in Majnoon oil field, southern Iraq," Iraqi Geological Journal, vol. 13, no. 1A, 2020.
- [8] M. A. Sarhan, T. Hassan, and A. S. Ali, "3D static reservoir modelling of Abu Madi paleo-valley in Baltim Field, Offshore Nile Delta Basin, Egypt," Petroleum Research, vo. 7, pp. 473-485, 2022.
- [9] J. M. Al Musawi, M. S. Al Jawad, "Study of different geostatistical methods to model formation porosity (Cast study of Zubair formation in Luhais oil field)," IOP Conf. Series: Materials Science and Engineering, vol. 579, 2019.
- [10] H. Wackernagel, "Geostatistical models and kriging," IFAC Proceedings Volumes, vol. 36, pp. 543-548, 2003.
- [11] M. J. Pyracz and C. V. Deutsch, "Geostatistical reservoir modeling," Oxford university press - New York, Second edition, p 116, 2014.
- [12] T. Buday, "The Regional Geology of Iraq, Stratigraphy, and Paleogeography," Dar Al Kutub Published house, Mosul, Iraq, pp. 445, 1980.

- [13] I. J. Hussein, "Building a Geological Model for the X oil field, Mishrif," M.Sc. Thesis, College of Engineering, University of Baghdad, 2012.
- [14] A. K. Alhusseini, and S. M. Hamd-Allah, "Estimation of Initial Oil in Place for X Oil Field by Using Volumetric Method and Reservoir Simulation Method," Iraqi Geological Journal, vol. 55, no. 2C, 2022.
- [15] M. M. Al-Ali, M. M. Mahdi and R. A. Alali, "Microfacies and depositional environment of Mishrif Formation, North Rumaila oil field, southern Iraq," Iraqi Geological Journal, vol. 52, no. 2, pp. 91-104, 2019.
- [16] T. A. Mahdi, A. A. M. Aqrabi, A. D. Horbury, and G. H. Sherwani, "Sedimentological characterization of the mid-Cretaceous Mishrif reservoir in southern Mesopotamian Basin, Iraq," GeoArabia, vol.18, no. 1, pp. 139-174, 2013.
- [17] M. M. Mohammed, H. M. Salih, and K. H. Mnaty, "3D Reservoir Modeling of Buzurgan Oil Field, Southern Iraq," Iraqi Journal of Science, vol. 63, no. 2, pp. 596-607, 2022.
- [18] M. Q. Aldarraji, and A. Z. Almayahi, "Seismic Structure Study of Buzurgan Oil field, Southern Iraq," Iraqi Journal of Science, vol. 60, no. 3, pp. 610-623, 2019.
- [19] M. H. Hakimi, and A. A. Al Ahmed, "Origin of crude oils from oilfields in the Zagros Fold Belt, Southern Iraq: Relation to organic matter input and paleoenvironmental conditions," Marine and Petroleum Geology, vol. 78, pp. 547-561. 2016.
- [20] Schlumberger, "Petrel introduction course," Schlumberger, pp.13-493, 2010.
- [21] B. A. Al-Baldawi, "Building A 3D Geological Model Using Petrel Software for Asmari Reservoir, South Eastern Iraq," Iraqi Journal of Science, vol.56, no.2C, pp.1750-1762, 2015.
- [22] S. J. Salman, "Three dimensions geostatistical model of the Mishrif carbonate reservoir of Amara oil field in Iraq," MSc thesis University of Baghdad, Collage of Engineering, Petroleum Engineering, 2015.
- [23] R. Olea, "A Practical Primer on Geostatistics ," U.S. Geological Survey Report, 2009.
- [24] T. Bai, and P. Tahmasebi, "Sequential Gaussian simulation for geosystems modeling: A machine learning approach," Geoscience Frontiers, vol. 13, 2022.
- [25] Schlumberger, "Petrel manual – property modeling methods," Schlumberger, 2009.
- [26] K. Robert, and P. Irakli, "Deterministic and stochastic methods of oilfield reserves estimation: a case study from Ka. Oilfield," 1st International Scientific Conference on Professional Sciences, Alexander Moisiu University, Durres, 2016.